17. Parker, M. A. Mutualism in metapopulations of legumes and rhizobia. *Am. Nat.* **153,** S48–S60 (1999).
18. De Jong, P. W., De Vos, H. & Nielsen, J. K. Demic structure and its relation with the distribution of an adaptive trait in Danish flea beetles. *Mol. Ecol.* **10,** 1323–1332 (2001).
19. Thompson, J. N. The evolution of species interactions. *Science* **284,** 2116–2118 (1999).
20. Thompson, J. N. & Pellmyr, O. Mutualism with pollinating seed parasites amid co-pollinators: constraints on specialization. *Ecology* **73,** 1780–1791 (1992).
21. Pellmyr, O. & Thompson, J. N. Sources of variation in pollinator contribution within a guild: the effects of plant and pollinator factors. *Oecologia* **107,** 595–604 (1996).
22. Caicco, S. L., Scott, J. M., Butterfield, B. & Csuti, B. A gap analysis of the management status of the vegetation of Idaho (U.S.A.). *Conserv. Biol.* **9,** 498–511 (1995).
23. Ricketts, T. H., Dinerstein, E., Olson, D. M. & Loucks, C. J. (eds) *Terrestrial Ecoregions of North America: A Conservation Assessment* (Island Press, Washington DC, 1999).
24. Pellmyr, O., Thompson, J. N., Brown, J. M. & Harrison, R. G. Evolution of pollination and mutualism in the yucca moth lineage. *Am. Nat.* **148,** 827–847 (1996).
25. Pellmyr, O. & Thompson, J. N. Multiple occurrences of mutualism in the yucca moth lineage. *Proc. Natl Acad. Sci. USA* **89,** 2927–2929 (1992).

### Acknowledgements

We thank D. Althoff, E. Bartlett, R. Beck, N. Bonilla, S. Bradford, C. Clark, C. Cody, M. Jacoby, S. Lambert, Y. Martinez, K. Merg, S. Nuismer, J. Olmstead, S. Ringo, K. Segraves, D. Shepard, Z. Stanley and T. Steury for help in the field or laboratory, and R. Calsbeek, D. Hembry, K. Horjus, R. Hufft, N. Janz, K. Merg, S. Nuismer and J. Richardson for helpful discussions on the manuscript. We are grateful for permissions from the Clearwater, Nez Perce, Payette, Salmon, and Umatilla National Forests and from the Turnbull National Wildlife Refuge. This work was supported by the NSF.

### Competing interests statement

The authors declare that they have no competing financial interests.

Correspondence and requests for materials should be addressed to J.N.T. (e-mail: thompson@biology.ucsc.edu).

# Spike train dynamics predicts theta-related phase precession in hippocampal pyramidal cells

**Kenneth D. Harris, Darrell A. Henze, Hajime Hirase, Xavier Leinekugel, George Dragoi, Andras Czurkó & György Buzsáki**

*Center for Molecular and Behavioral Neuroscience, Rutgers, The State University of New Jersey, 197 University Avenue, Newark, New Jersey 07102, USA*

**According to the temporal coding hypothesis[1], neurons encode information by the exact timing of spikes. An example of temporal coding is the hippocampal phase precession phenomenon, in which the timing of pyramidal cell spikes relative to the theta rhythm shows a unidirectional forward precession during spatial behaviour[2,3]. Here we show that phase precession occurs in both spatial and non-spatial behaviours. We found that spike phase correlated with instantaneous discharge rate, and precessed unidirectionally at high rates, regardless of behaviour. The spatial phase precession phenomenon is therefore a manifestation of a more fundamental principle governing the timing of pyramidal cell discharge. We suggest that intrinsic properties of pyramidal cells have a key role in determining spike times, and that the interplay between the magnitude of dendritic excitation and rhythmic inhibition of the somatic region is responsible for the phase assignment of spikes[4,5].**

Two competing frameworks have been suggested for the representation of information in the brain: rate coding and temporal coding. Rate coding suggests that information is represented by discharge rates over a group of neurons[6]. Temporal coding models, on the other hand, argue that the temporal relationship of spikes is more critical for information transfer[7–11]. During spatial behaviours, hippocampal pyramidal neurons discharge specifically at certain locations in the environment (the 'place field'), implying that hippocampal neurons 'code' for spatial information[12]. Furthermore, phase assignment of spikes with respect to the theta rhythm shows a unidirectional advancement as the animal crosses the place field[2,3]. Because spike phase shows a monotonic relation to position, whereas firing rate increases and decreases as the animal enters and leaves the place field, it was suggested that this 'temporal code' might be a reliable mechanism for representing space[2,13].

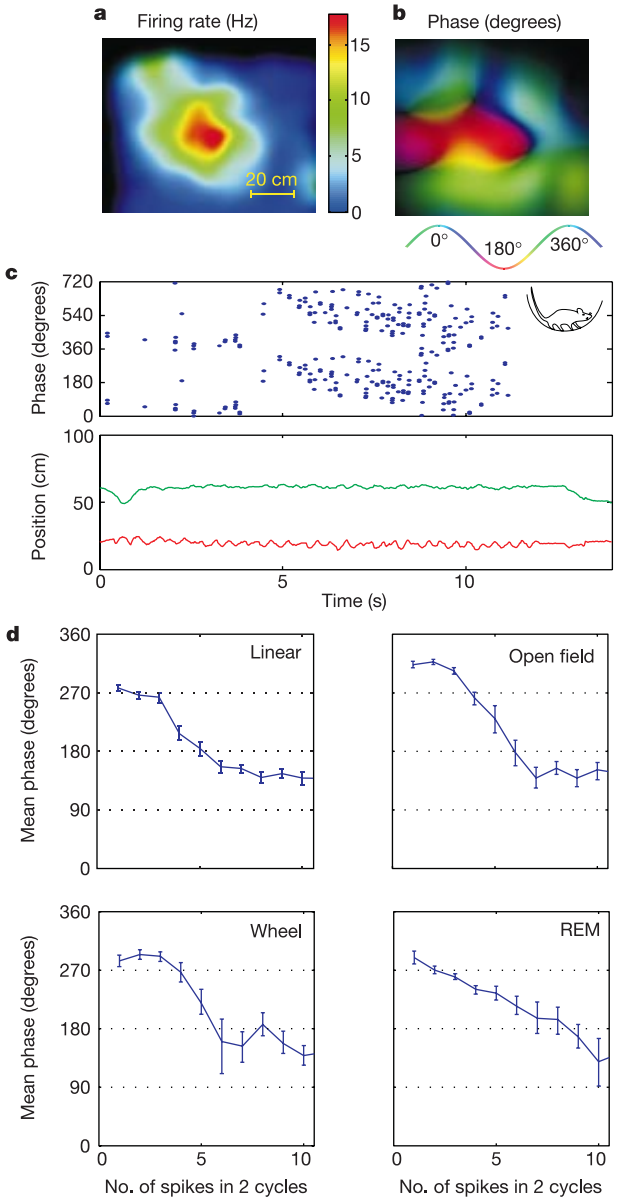


**Figure 1** Relation between theta phase and instantaneous firing rate in pyramidal cells. **a**, Mean firing rate as a function of position, for an illustrative CA1 pyramidal cell ('place map'). **b**, Mean firing phase as a function of position for the same cell ('phase map'). **c**, Spike phase advancement during a wheel running episode. The cell fired sparsely at constant phase until 5 s into the trial, when an intense period of firing occurred, accompanied by phase precession, although the rat's head remained stationary (<3 cm). Top panel, phase and time of spikes. Bottom panel, instantaneous head position (red and green: *X* and *Y* coordinates). **d**, Rate versus phase relationship during four types of behaviour. For each spike, instantaneous rate was estimated by the number of spikes in the 720° interval centred on it. Graph shows circular mean and 95% confidence interval[23] of all spikes in the database, grouped by instantaneous rate. Phase 0 corresponds to the positive peak of CA1 pyramidal layer theta. The database consisted of 28, 181, 23 and 253 cells from 3, 5, 7 and 15 rats in the linear, open field, wheel and REM behaviours.

A critical issue is whether phase precession is explicitly tied to spatial computations, or arises from a more general mechanism. We suggest that hippocampal phase advancement has a cellular origin, owing to a dependence of preferred phase on the strength of dendritic depolarization[4,5]. If this is the case, phase precession effects should be seen in both spatial and non-spatial behaviours. Here we address this issue by investigating the relation of phase to spike train dynamics, independent of continuing behaviour.

Figure 1a and b shows the two-dimensional place field and 'phase field' of a representative pyramidal cell during spatial exploration in an open field, showing the firing rate and mean phase of firing with respect to CA1 pyramidal layer theta at each point in space. In agreement with previous investigations[2,3], both firing rate and phase correlated with the spatial coordinates of the animal. In agreement with the depolarization hypothesis, the spatial dependence of firing phase largely mirrored that of firing rate, with mean phase in the centre of the place field being advanced compared to the periphery. An example of phase precession during a non-spatial behaviour (wheel running) is shown in Fig. 1c, where again phase precession was seen at times of high firing rate.

To investigate the phase–firing rate relationship quantitatively and independently of the spatial position of the rat (Fig. 1d), we examined the phase of spikes during linear track running ($n = 28$ cells), open field exploration ($n = 181$), wheel running with stationary head ($n = 23$), and REM sleep ($n = 253$). Instantaneous firing rate was quantified for each spike by counting the number of spikes up to 360° of theta before and after the spike whose rate was to be quantified. For each behavioural category, the effect of firing rate on phase was significant ($P < 0.001$; circular analysis of variance (ANOVA) on all spikes for each behaviour; see Supplementary Information). Mean phase, averaged over all behaviours, shifted from 295° ± 7° (circular mean ± 95% confidence interval) at low instantaneous rates (1 spike per 2 cycles; ~4 Hz) to 141° ± 9° for high rates (≥10 spikes per 2 cycles; ~40 Hz). CA3 pyramidal cells recorded in linear track running ($n = 54$) and open field ($n = 74$) showed a similar relationship, although the phase of firing (relative to CA1 pyramidal layer theta) was earlier at both low and high firing rates (overall mean 258° ± 15° and 96° ± 25°). As a further test of the proposed depolarization–phase relationship, we examined the relationship of spike phase on extracellular amplitude, which has been observed to decrease at times of strong activity[14,15]. In each behavioural category, spike phase advanced robustly as the amplitude decreased (Supplementary Information).

A phase–firing rate correlation therefore exists in both spatial and non-spatial behaviours. Nevertheless, this correlation may not fully summarize the phase dynamics of pyramidal cells. In spatial behaviours, phase shift occurs unidirectionally over multiple theta cycles[2,3]. Do spike trains in non-spatial behaviours show a similar tendency? Unidirectional phase advancement implies that the phase of spikes advances between the onset and the cessation ('offset') of periods of firing. On a linear track, firing onset and offset reliably occur in distinct spatial locations, and unidirectional advancement may therefore be detected by correlating phase with position. However, this analysis cannot be used in other behaviours. We therefore classified spikes as corresponding to firing onset and offset directly. Spikes were classified as belonging to an accelerating spike

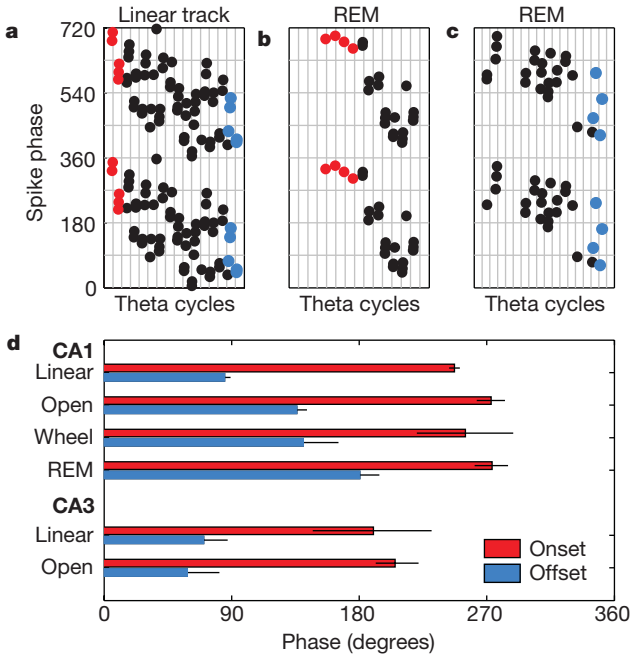


**Figure 2** Unidirectional nature of the phase shift. **a**–**c**, Subsets of spikes were selected as occurring at the onset (red) or offset (blue) of activity (see text). Most spikes (black) met neither criterion. The graphs show the results of the selection process on example spike trains from three single units. Out of a grand total of 301,693 spikes, 7,750 were selected as onset and 7,277 as offset. Vertical lines, successive theta cycles. **d**, For each behaviour, the circular mean phase and 95% confidence interval was calculated for all spikes in the database classified as onset (red) or offset (blue). For CA1, number of cells and rats same as Fig. 1. For CA3, 54 and 74 cells from 1 rat in the linear track and open field behaviour.

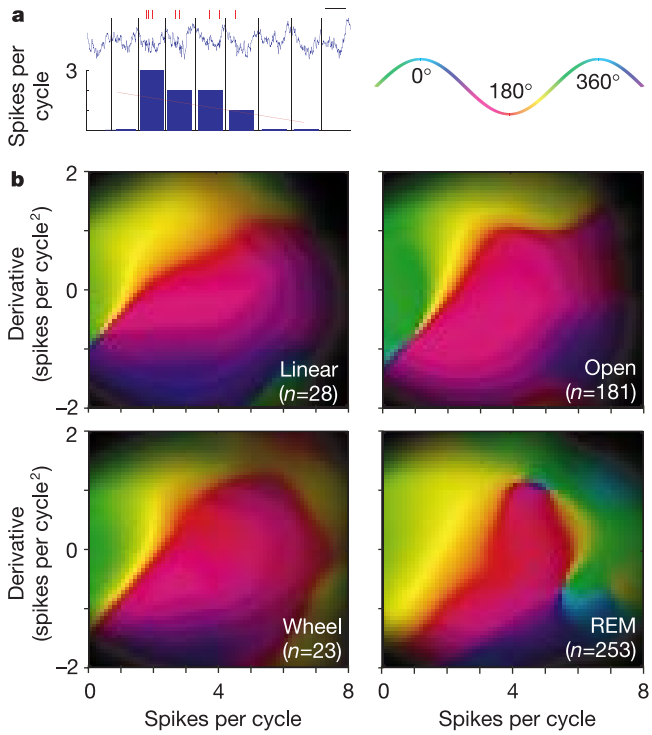


**Figure 3** Mean phase as a function of instantaneous rate and its temporal derivative. **a**, Calculation of rate derivative. Top, theta oscillation (blue) and spike times (red ticks) in an example data segment. Scale bar, 100 ms. Bottom, the temporal derivative of discharge rate for each cycle was calculated by linear regression of spike count (blue bars) against cycle number in a seven-cycle window (red line). **b**, Pseudo-colour plots showing phase as a function of instantaneous rate and its derivative, averaged over all spikes in the database, for each behaviour. Rate derivative begins to influence spike phase at rates >1 spike per theta cycle (~8 Hz). Number of cells and rats same as Fig. 1.

train (onset) if the previous 8 theta cycles contained at most 4 spikes, and the following 8 contained at least 16 (an increase from <4 Hz to >16 Hz, assuming 8-Hz theta), and to a decelerating train (offset) if the previous 8 cycles contained at least 16, and the next at most 4 (Fig. 2a–c). The mean phase was significantly earlier for spikes in decelerating patterns than for accelerating patterns in all four behaviours (Fig. 2d; $P < 0.001$; Mardia-Watson-Wheeler test; Supplementary Information).

Is the unidirectional nature of phase precession explained simply by lower firing rates at activity onset, or can it occur even in the absence of firing rate change? To address this question, we considered the dependence of phase on both rate and its instantaneous temporal derivative (Fig. 3a, b). At low firing rates (≤0.25 spikes per cycle, ~2 Hz), there was little effect of rate derivative (mean of all spikes in combined behaviours ±95% confidence interval: 317° ± 12°; green on Fig. 3b). At higher rates (>1 spike per cycle, ~8 Hz), mean spike phase depended on the combined effect of rate and the derivative of rate, advancing further as acceleration (mean of all spikes with derivative ≥1 spike per cycle$^2$, 267° ± 28°; yellow), turned to deceleration (mean of all spikes with derivative <1 spike per cycle$^2$, 92° ± 26°; mauve). The example of Fig. 1c is therefore illustrative of mean behaviour: at low rates, phase is constant, and unidirectional advancement occurs only at times of intense activity[16].

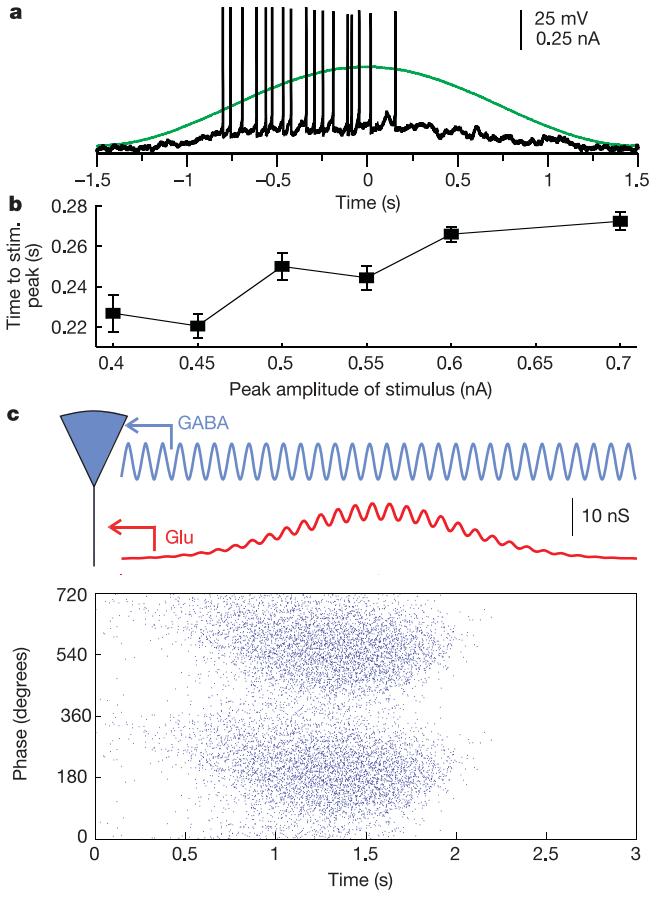


**Figure 4** Proposed role of adaptation in unidirectional phase precession. **a**, Symmetrical ramp currents (green line), were injected into the soma of hippocampal pyramidal neurons of anaesthetized rats. More spikes occurred on the ascending than descending part of the ramp, and peak firing preceded the depolarization peak. **b**, The forward shift between peak firing rate and maximum depolarization increased with the amount of depolarization. Each point shows mean and standard error of 50 repetitions from one cell. **c**, Soma-dendritic interference (SDI) model of phase precession. A compartmental model pyramidal cell experienced a sinusoidal $Cl^-$ conductance at the soma (mimicking $GABA_A$ receptor-mediated inhibition), and a sinusoidal dendritic $Na^+$ conductance (mimicking glutamate excitation, Glu), modulated by a symmetrical drive function. The graph shows phase versus time for the overlaid spikes of 100 model runs. Owing to adaptation, the model ceased firing before the offset of excitation, and showed unidirectional phase advance.

The finding that phase advancement occurs only at times of high firing rate supports the hypothesis that phase precession is a function of excitation strength. According to this hypothesis, phase modulation occurs due to an 'interference' effect between rhythmic somatic inhibition and dendritic excitation (soma-dendritic interference or SDI model)[4,5]. At times of weak drive, inhibition dominates, and the cell fires when it is least inhibited (the positive phase). At times of strong drive, excitation dominates, and the cell fires when it is most excited (the negative phase). This interference mechanism may also explain the unidirectional nature of phase precession, given a further assumption that, owing to adaptation, the firing rate begins to decrease before the strength of dendritic excitation has reached its peak. Under this assumption, the onset of spiking activity will occur at the same time as the onset of excitation, but the offset of spiking will occur before the offset of excitation. Accordingly, dendritic depolarization will be larger at the offset of spiking than at the onset, and phase will be advanced.

This hypothesis was investigated in two ways. First, temporally symmetric current ramps were injected into CA1 and CA3 pyramidal cells of anaesthetized rats ($n = 18$; Fig. 4a, b). The resulting spike trains showed 2.6 ± 0.7 times more spikes on the ascending than the descending part of the ramp, supporting the hypothesis that firing rate begins to decline before the offset of excitation. Furthermore, the degree of asymmetry increased with increasing amount of depolarization. Second, a compartmental model pyramidal cell (Fig. 4c; see Methods) was subjected to a sinusoidal somatic $Cl^-$ conductance together with a sinusoidal dendritic $Na^+$ conductance. The latter was modulated by a symmetrical ramp function, simulating a place field traversal. The model exhibited a dependence of preferred phase on excitation strength. In addition, because of adaptation, firing offset occurred before excitation offset, and a unidirectional phase advance was seen, similar to place field traversals *in vivo*[2,3].

In summary, in both spatial and non-spatial behaviours, timing of hippocampal pyramidal cells within the theta cycle shows a correlation with instantaneous firing rate, and exhibits unidirectional phase precession at rates exceeding one spike per cycle. Similar phase precession was produced by a SDI model, in which phase was determined by the relative magnitude of oscillatory inhibitory somatic and excitatory dendritic inputs. We propose that the SDI mechanism has an important role in coordinating the timing of hippocampal cell populations, and that this temporal organization is fundamental to processing of both spatial and non-spatial information in the hippocampus. □

## Methods

Fifteen male rats were implanted with movable tetrodes. Before implantation, seven rats were trained to run continuously in a running wheel for water reinforcement available in an adjacent box. The remaining eight animals were recorded either while exploring in a large rectangular box (1.2 m × 1.2 m × 0.5 m high) or walking on an elevated square track (65 cm side length; 8.5 cm wide 'linear' track) for chocolate reward. An infrared LED was attached to the head stage to track the position of the animal. Sleep recordings were carried out in the home cage of the rat. To ensure stationarity, the first and last seconds of wheel running epochs were excluded. Electrode placement was localized histologically[17]. Extracellular spikes were extracted from the traces by previously described methods[18,19]. Only sufficiently well-isolated units were considered for analysis (isolation distance ≥20)[15]. Theta activity was detected by calculating the ratio of the Fourier components of the theta (5–10 Hz) and delta (2–4 Hz) frequency band[20]. Intracellular experiments were performed in urethane anaesthetized rats[21], with intracellular injection of symmetrical triangular or sinusoid waveforms (3 s long).

Local field potentials recorded in the CA1 pyramidal layer were digitally filtered for theta (4–10 Hz). Spike phase was calculated using a Hilbert transform. 'Phase fields' were calculated by a locally weighted circular mean using a gaussian smoothing function of width 7.5 cm. To compute the derivative of firing rate, a linear regression was performed for the number of spikes per cycle as a function of cycle number, using the central and three

neighbouring cycles on each side. The derivative and instantaneous firing rate were estimated as the slope of the fit line, and its intercept in the central cycle. Circular ANOVA was performed using the test statistic $\sum \cos(\theta_i - \bar{\theta}_{g(i)})$, where $\bar{\theta}_{g(i)}$ is the circular mean for the group to which observation $i$ is assigned. The null distribution was computed by 1,000-fold random reassignment of groups.

Computational simulations were performed in NEURON (http://www.neuron.yale.edu) using a two-compartment model of a hippocampal pyramidal cell. Conductance and calcium dynamics were as described by Migliore[22]. Compartment geometry: soma length 50 μm, diameter 40 μm, dendrite length 50 μm, diameter 3.3 μm. Somatic peak channel conductances (S cm$^{-2}$): $G_{Na}$ 0.015; $G_K$(DR) (delayed rectifier) 0.009; $G_K$(A) (A-type) 0.0001; $G_K$(M) (M-type) 0.00002; $G_K$(AHP) (after-hyperpolarization) 0.004; $G_{Ca}$(L) (L-type) 0.0025; $G_{Ca}$(N) (N-type) 0.0025; $G_{Ca}$(T) (T-type) 0.00025; dendritic same without $G_{Na}$. 10-Hz sinusoidal conductances were added to the soma ($Cl^-$, peak 20 nS at 120°, phase modulation 50%) and dendrite ($Na^+$, peak 15 nS at 180°, phase modulation 30%). Modulation depth and preferred phase were based on extracellular recordings of interneurons and pyramidal cells *in vivo*[20]. The dendritic current was further modulated by a gaussian function of time (width 500 ms). Synaptic noise was added at the dendrite ($Na^+$, Poisson process, mean rate 1 kHz, peak conductance 5 nS).

Received 8 November 2001; accepted 2 April 2002; doi:10.1038/nature00808.


1. Singer, W. Synchronization of cortical activity and its putative role in information processing and learning. *Annu. Rev. Physiol.* **55,** 349–374 (1993).
2. O'Keefe, J. & Recce, M. L. Phase relationship between hippocampal place units and the EEG theta rhythm. *Hippocampus* **3,** 317–330 (1993).
3. Skaggs, W. E., McNaughton, B. L., Wilson, M. A. & Barnes, C. A. Theta phase precession in hippocampal neuronal populations and the compression of temporal sequences. *Hippocampus* **6,** 149–172 (1996).
4. Magee, J. C. Dendritic mechanisms of phase precession in hippocampal CA1 pyramidal neurons. *J. Neurophysiol.* **86,** 528–532 (2001).
5. Kamondi, A., Acsady, L., Wang, X. J. & Buzsaki, G. Theta oscillations in somata and dendrites of hippocampal pyramidal cells in vivo: activity-dependent phase-precession of action potentials. *Hippocampus* **8,** 244–261 (1998).
6. Adrian, E. D. & Zotterman, Y. The impulses produced by sensory nerve endings. Part 2. The response of a single end organ. *J. Physiol. (Lond.)* **61,** 151–171 (1926).
7. Gray, C. M. & Singer, W. Stimulus-specific neuronal oscillations in orientation columns of cat visual cortex. *Proc. Natl Acad. Sci. USA* **86,** 1698–1702 (1989).
8. Hopfield, J. J. Pattern recognition computation using action potential timing for stimulus representation. *Nature* **376,** 33–36 (1995).
9. Buzsaki, G. & Chrobak, J. J. Temporal structure in spatially organized neuronal ensembles: a role for interneuronal networks. *Curr. Opin. Neurobiol.* **5,** 504–510 (1995).
10. Vaadia, E. *et al.* Dynamics of neuronal interactions in monkey cortex in relation to behavioural events. *Nature* **373,** 515–518 (1995).
11. Riehle, A., Grun, S., Diesmann, M. & Aertsen, A. Spike synchronization and rate modulation differentially involved in motor cortical function. *Science* **278,** 1950–1953 (1997).
12. O'Keefe, J. & Nadel, L. *The Hippocampus as a Cognitive Map* (Clarendon, Oxford, 1978).
13. Burgess, N., Recce, M. & O'Keefe, J. A model of hippocampal function. *Neural Networks* **7,** 1065–1081 (1994).
14. Quirk, M. C., Blum, K. I. & Wilson, M. A. Experience-dependent changes in extracellular spike amplitude may reflect regulation of dendritic action potential back-propagation in rat hippocampal pyramidal cells. *J. Neurosci.* **21,** 240–248 (2001).
15. Harris, K. D., Hirase, H., Leinekugel, X., Henze, D. A. & Buzsaki, G. Temporal interaction between single spikes and complex spike bursts in hippocampal pyramidal cells. *Neuron* **32,** 141–149 (2001).
16. Hirase, H., Czurko, A., Csicsvari, J. & Buzsaki, G. Firing rate and theta-phase coding by hippocampal pyramidal neurons during 'space clamping'. *Eur. J. Neurosci.* **11,** 4373–4380 (1999).
17. Csicsvari, J., Hirase, H., Mamiya, A. & Buzsaki, G. Ensemble patterns of hippocampal CA3-CA1 neurons during sharp wave-associated population events. *Neuron* **28,** 585–594 (2000).
18. Csicsvari, J., Hirase, H., Czurko, A. & Buzsaki, G. Reliability and state dependence of pyramidal cell-interneuron synapses in the hippocampus: an ensemble approach in the behaving rat. *Neuron* **21,** 179–189 (1998).
19. Harris, K. D., Henze, D. A., Csicsvari, J., Hirase, H. & Buzsaki, G. Accuracy of tetrode spike separation as determined by simultaneous intracellular and extracellular measurements. *J. Neurophysiol.* **84,** 401–414 (2000).
20. Csicsvari, J., Hirase, H., Czurko, A., Mamiya, A. & Buzsaki, G. Oscillatory coupling of hippocampal pyramidal cells and interneurons in the behaving rat. *J. Neurosci.* **19,** 274–287 (1999).
21. Henze, D. A. & Buzsaki, G. Action potential threshold of hippocampal pyramidal cells in vivo is increased by recent spiking activity. *Neuroscience* **105,** 121–130 (2001).
22. Migliore, M., Cook, E. P., Jaffe, D. B., Turner, D. A. & Johnston, D. Computer simulations of morphologically reconstructed CA3 hippocampal neurons. *J. Neurophysiol.* **73,** 1157–1168 (1995).
23. Fisher, N. I. *Statistical Analysis of Circular Data* (Cambridge Univ. Press, New York, 1993).


**Supplementary Information** accompanies the paper on *Nature*'s website (http://www.nature.com/nature).


## Acknowledgements

This work was supported by the NIH and the Human Frontier Science Program.


## Competing interests statement

The authors declare that they have no competing financial interests.

Correspondence and requests for materials should be addressed to G.B. (e-mail: buzsaki@axon.rutgers.edu).

# Role of experience and oscillations in transforming a rate code into a temporal code

**M. R. Mehta, A. K. Lee & M. A. Wilson**

*Center for Learning & Memory, Department of Brain & Cognitive Sciences, RIKEN-MIT Neuroscience Research Center, Massachusetts Institute of Technology, Cambridge, Massachusetts 02139, USA*

**In the vast majority of brain areas, the firing rates of neurons, averaged over several hundred milliseconds to several seconds, can be strongly modulated by, and provide accurate information about, properties of their inputs. This is referred to as the rate code. However, the biophysical laws of synaptic plasticity require precise timing of spikes over short timescales (<10 ms)[1,2]. Hence it is critical to understand the physiological mechanisms that can generate precise spike timing *in vivo*, and the relationship between such a temporal code and a rate code. Here we propose a mechanism by which a temporal code can be generated through an interaction between an asymmetric rate code and oscillatory inhibition. Consistent with the predictions of our model, the rate[3,4] and temporal[5–7] codes of hippocampal pyramidal neurons are highly correlated. Furthermore, the temporal code becomes more robust with experience. The resulting spike timing satisfies the temporal order constraints of hebbian learning. Thus, oscillations and receptive field asymmetry may have a critical role in temporal sequence learning.**

We recorded the activity of pyramidal neurons from the dorsal CA1 region of the hippocampus in awake, behaving rats (see Methods). The firing rate of these neurons depends on the spatial location of the rat[3], and hence these neurons are referred to as 'place cells'. The mean firing rates (averaged over >200 ms) of about 100 neurons can provide an accurate estimate of the rat's spatial location[4]. This is the hippocampal rate code.

In addition to this spatial parameter, hippocampal activity during active exploration is strongly modulated by a temporal parameter, namely the 8-Hz theta rhythm. In a classic study, O'Keefe and Recce showed that[5,6] the phase of the theta rhythm at which a place cell fires a spike steadily precesses to lower values as the rat moves further along the place field (Fig. 1a). Consistent with this, phase was highly (negatively) correlated with position ($r = -0.50 \pm 0.01$, $P < 0.0001$) across 171 recorded place fields (henceforth referred to as the 'population'). Normalizing by occupancy (see Methods) yields the firing rate as a function of position and phase—that is, the spatio-temporal receptive field (STRF, Fig. 1b). The firing rate increases as phase decreases (from 360° to 180°) and position increases, reaching a maximal value at a position beyond the centre (white line) of the place field and at 200° (red arrow) towards the end of the place field: that is, the firing rate is an inseparable function of high phases (180° < phase < 360°) and position. The firing rate at low phases (0° < phase < 180°) shows a weaker dependence on phase and position.

The vast majority of neurons have a similar spatio-temporal structure (as Fig. 1b), in which the firing rate shows a significant increase as the mean phase decreases and the distance within the place field increases (population average, Fig. 1c, d). Thus, there is spatial information in the precise timing of spikes (accurate up to 10 ms) with respect to the theta rhythm[5–7]. This is the hippocampal temporal code, which has several advantages over the rate code, such as insensitivity to the rat's running speed[5] and scale invariance[7].

Several computational models have been proposed to explain the origin of this temporal code[5,8–11]. These models were based upon the